Enhancing Ship Generator Reliability by Modifying Bearings to Prevent Electrical Arcing Damage

Rukmini
Ship Machinery, Politeknik Pelayaran Barombong, Sulawesi Selatan, Indonesia
rukmini@poltekpelbarombong.ac.id (corresponding author)

Antoni Arif Priadi
Nautical, Sekolah Tinggi Ilmu Pelayaran, Jakarta, Indonesia
antoni.kemenhub@gmail.com

Azwar Hayat
Mechanical Engineering, Universitas Hasanuddin, Sulawesi Selatan, Indonesia
azwar.hayat@unhas.ac.id

Received: 12 May 2025 | Revised: 25 October 2025 | Accepted: 3 November 2025

 DOI: https://doi.org/10.48084/etasr.12085

ABSTRACT

Stray electrical currents in marine generators cause catastrophic bearing fluting, leading to frequent failures and operational downtime. The harsh maritime environment exacerbates this issue, demanding a more robust solution than conventional methods. This study introduces an innovative porcelain insulation sleeve applied to the bearing housing of a 250 kVA ship generator. Its effectiveness was evaluated through comparative in-situ testing, measuring vibration, temperature, and electrical parameters under a 22 kW load, with insulation thicknesses varying from 2.0 mm to 2.75 mm. The porcelain armor performed exceptionally. A 2.20 mm thickness was identified as optimal, achieving a 94% reduction in vibration and a 3.7 °C drop in operating temperature. Critically, the insulation's ultra-high insulation resistance (1000 GΩ) completely blocked the path of parasitic currents, eliminating the root cause of electrical arcing and fluting damage. This work demonstrates that applying porcelain insulation provides a definitive, maintenance-free solution to bearing fluting. The research validates a highly effective and practical engineering intervention that significantly enhances the reliability, safety, and service life of marine generators.

Keywords-bearing current mitigation; marine generator reliability; porcelain insulation armor; fluting damage prevention; in-situ vibration analysis

I. INTRODUCTION

Bearing current is a destructive phenomenon in low-voltage marine generators (380 V/50 Hz or 440 V/60 Hz), initiated by the circulation of harmonic currents from the stator to the rotor through the bearings [1-4]. These currents cause electrical discharges that damage bearing surfaces and lead to operational failures such as fluting, pitting, and rapid lubricant degradation [5-10]. Ultimately, this condition can result in insulation failure and unplanned generator downtime [11].

The operational challenges associated with this issue are significant. They include premature bearing wear, diminished lubrication effectiveness, elevated operating temperatures, and unexpected generator failures, even with routine maintenance [11]. Contributing factors exacerbating these problems are the harsh marine environment, poor power quality, and the use of self-excitation systems that are highly susceptible to voltage fluctuations and harmonic distortion. Furthermore, non-linear loads worsen voltage regulation distortion, thereby increasing the risk of electrical discharges across the bearings [12]. As a result, the impact of this damage is multidimensional. It not only drastically compromises system reliability but also escalates maintenance costs and jeopardizes vessel operational safety [13]. In worst-case scenarios, bearing failure can precipitate stator winding failure or even catastrophic generator breakdown [14], as illustrated in Figures 1 and 2.

While various mitigation strategies have been established for industrial motors, a significant research gap remains concerning robust and durable solutions for low-voltage marine generators [12]. Existing studies frequently overlook the unique combination of the electromechanical and environmental stresses inherent to marine operations [11].

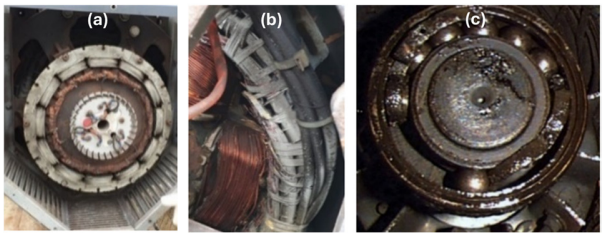

Fig. 1. Generator failure caused by bearing failure, showing: (a) front view, (b) burnt stator coil, and (c) damaged roller bearing.

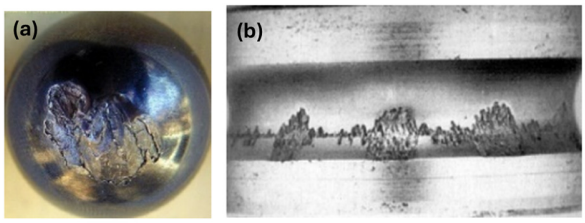

Fig. 2. Condition of damaged ball bearings and raceways: (a) torn ball bearings and (b) scratches on the raceways.

In this context, porcelain insulation emerges as a highly promising solution due to its exceptional dielectric strength (up to 3000 V/mm) [15], mechanical resistance, and durability against environmental degradation. These properties make it an ideal candidate for marine applications requiring effective and long-lasting bearing current mitigation.

Given the urgency of the problem, this study aims to propose and validate the effectiveness of porcelain insulation in preventing bearing damage caused by electrical surges in ship generators. The scope is limited to a 250 kVA, low-voltage generator operating under controlled load conditions, utilizing bearings with dimensions of 90 mm x 160 mm x 30 mm, as proposed by SKF. The evaluation will focus on the application of porcelain insulation samples, approximately 2 mm thick, applied to the bearing housing, as shown in Figure 3.

Fig. 3. Porcelain insulation application process on the bearing outer cover.

Specifically, the research is designed to answer three primary questions:

1. How does porcelain insulation thickness affect bearing vibration levels and operating temperature?
2. To what extent can this insulation prevent electrical sparking and fluting?
3. What is the practical feasibility of its application in marine systems?

1) Fundamental Mechanism of Bearing Current Generation

The generation of bearing currents in electric machines is a complex issue stemming from the use of power electronic converters. The core of the problem lies in two interrelated physical phenomena [16], capacitive coupling between the stator and rotor, and the high-frequency Common-Mode Voltage (CMV) generated by the converter [17-20]. This CMV induces parasitic currents that seek the path of the least impedance to ground. Within the machine's structure, the bearings often become this unintended path, as their impedance can be lower than the designed grounding path.

Based on their generation mechanism and flow characteristics, bearing currents can be classified into three main types:

a) Capacitive Bearing Current

This current results directly from the electrical potential difference between the rotor and stator, forming a capacitive circuit through the bearing's rolling elements. It is characterized by a continuous flow with relatively low amplitude. The current magnitude can be modeled and predicted using the Bearing Voltage Ratio (BVR) parameter [21, 22]. This parameter is highly dependent on the magnitude of the parasitic capacitance between internal machine components [23], as illustrated in Figure 4. The *BVR* parameter is defined as:

$$V_{com} = \frac{V_A+V_B+V_C}{3} \quad (1)$$

$$BVR = \frac{V_b}{V_{com}} = \frac{C_{wr}}{C_{wr}+C_{rf}+2C_b} (assume\ C_{b1} = C_{b2} = C_b) \quad (2)$$

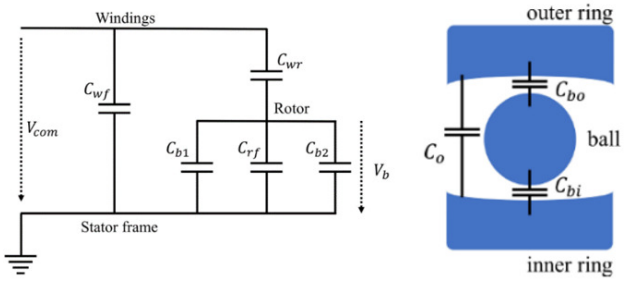

Fig. 4. Standard mode capacitive coupling circuit.

b) Electrical Discharge Machining (EDM)-i.

Electrical Discharge Machining (EDM) current occurs when the voltage across the bearing gap surpasses the dielectric strength of the lubricant film. This event triggers a concentrated, impulsive electrical discharge, leading to localized thermal erosion, the formation of microscopic craters, and progressive degradation of the bearing raceways and rolling elements [23]. This phenomenon is analogous to the controlled erosion process used in EDM.

c) Circulating Bearing Current and Rotor Ground Current

These currents are induced by magnetic asymmetries in the air gap or imbalances in ground impedance. Circulating currents form a closed-loop path through the shaft, both bearings, and the stator frame. In contrast, rotor ground

currents flow due to insufficient insulation between the rotor and ground, particularly in machines with low-impedance paths to the frame [24, 25], as depicted in Figure 5.

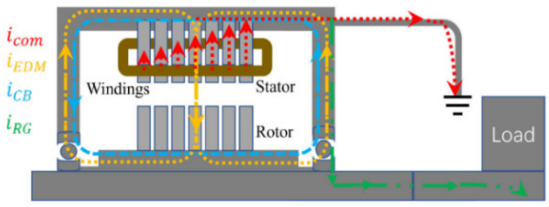

Fig. 5. Bearing current loop diagram.

2) Destructive Impacts and Evaluation of Conventional Mitigation Strategies

Electric current flow through bearings has cumulative and detrimental effects, substantially diminishing operational reliability and increasing maintenance demands, especially in harsh marine environments. The primary impact occurs within the lubricant. The high temperatures and electrical stress from the current degrade the grease's molecular structure, reducing its viscosity and dielectric strength. This deterioration of the lubricant's insulating properties facilitates increased current flow, creating a positive feedback loop that accelerates damage [26-29].

The dominant damage mechanism is the EDM effect, where microscopic discharges concentrate energy, locally vaporizing the bearing steel. The cumulative result produces characteristic damage patterns, such as frosting, a dull surface finish from widespread micro-pitting and fluting, a washboard-like erosion pattern perpendicular to the direction of rotation caused by systematic discharges at rolling element passing frequencies [30-32]. This damage precipitates premature bearing failure. The resulting vibration can induce misalignment, damage secondary components like stator windings, and lead to unplanned downtime with significant associated repair costs [7, 16]. Consequently, mitigating bearing currents is not merely a maintenance activity but an essential requirement for ensuring system reliability and reducing the total cost of ownership. Conventional mitigation strategies primarily focus on two approaches. The first involves shaft grounding devices, such as brushes or rings, which provide a low-impedance path to bypass current away from the bearings. The second employs insulated bearings, typically featuring ceramic (e.g., alumina oxide) rolling elements or rings, designed to block the current path entirely [33, 34]. To understand why these mitigation strategies are necessary, it is important to consider the damage mechanism. When current flowing through a bearing generates electrical sparks, which in turn excite mechanical vibrations. In bearing vibration analysis, it is essential to understand the underlying concepts. Specifically, vibration signals comprising periodic transient impulses can be mathematically represented by [35]:

$$X(t) = Ae^{-2\Lambda cft}\cos(2\pi ft) \quad (3)$$

$$X_1(t) = e^{0.06.2\pi.150t}\sin\left(\sqrt{1-0.06^2}.2\pi.150t\right) \quad (4)$$

where $X(t)$ is the vibration signal, $X_1(t)$ is the time domain wave, A is the amplitude, t is the time ($t \geq 0$), f is the frequency, and c is the damping characteristic controller.

A critical evaluation, however, reveals significant limitations of both conventional methods in maritime environments. Grounding devices are prone to mechanical wear, fouling, and contamination from oil, dust, and salt, necessitating frequent maintenance. Insulated bearings, meanwhile, are costly and susceptible to cracking from thermal cycling and mechanical shock.

3) Porcelain as an Innovative Insulation Solution

Based on the identified gaps in existing methods, this study proposes an alternative solution: applying a porcelain insulation layer to the generator's bearing housing. To evaluate this approach, experiments were conducted using porcelain layers of varying thicknesses. The selection of porcelain is grounded in its strong theoretical merits and proven performance history. As a high-temperature-fired inorganic material, porcelain possesses a composite structure of glass and crystalline phases that confers superior properties: very high dielectric strength (typically >30 kV/mm) [15], excellent volume resistivity, and exceptional mechanical hardness (>1500 Vickers Hardness Number) [34, 36].

The functional properties of porcelain are derived from the distinct and complementary roles of its constituent materials during processing and firing. Kaolin ($Al_2Si_2O_5(OH)_4$) imparts essential plasticity for the forming stage and subsequently evolves into the primary structural matrix upon firing. This skeletal framework is then bonded by Feldspar (e.g., $KAlSi_3O_8$), which acts as a fluxing agent that lowers the vitrification temperature by forming a continuous glassy phase, thereby consolidating the structure and significantly reducing porosity. Concurrently, Quartz (SiO_2) particles serve as a robust filler material, providing key structural reinforcement and counteracting volumetric shrinkage throughout the firing process to ensure dimensional stability.

The specific porcelain type considered suitable for this bearing application is hard porcelain, with a base composition in the K_2O–Al_2O_3–SiO_2 system, formulated from Kaolin, Feldspar, and Quartz. This formulation has a demonstrated history of effectiveness in high-performance insulation applications [36-39].

This material has been the established standard for high-voltage insulators on power transmission lines for decades, proving its robust endurance under extreme environmental conditions, including UV radiation, high humidity, and wide thermal fluctuations [37]. For marine generators, these properties translate into distinct advantages: porcelain offers a passive, permanent, and maintenance-free insulating barrier. Its inherent hardness provides excellent resistance to abrasion and mechanical stress, while its chemical inertness ensures immunity to lubricants, moisture, and corrosive marine atmospheres [39].

Therefore, integrating porcelain insulation directly into the bearing housing design promises a solution that is inherently more robust against the common failure modes of conventional

methods, potentially yielding a significant improvement in marine generator reliability.

II. METHOD

A comprehensive experimental framework was designed to evaluate the effectiveness of porcelain insulation on generator bearings under real-world operational conditions. The study employed a rigorous before-and-after (A-B) experimental design to isolate and quantify the effect of the insulation intervention. The investigation was conducted in situ on Generator 2 aboard the MT. Hasanuddin Training Vessel, operated by the Merchant Marine Polytechnic of Makassar. The unit under test was a 250 kVA marine generator (22 kW, 380 V, 1500 rpm), as displayed in Figure 7.

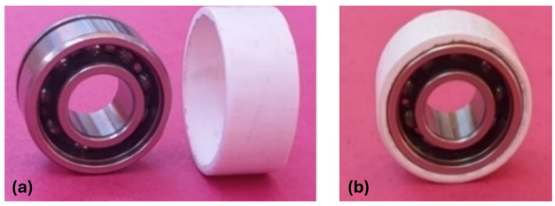

Fig. 6. Bearing assembly states: (a) standard ball bearing without porcelain insulation and (b) ball bearing integrated with a porcelain insulation sleeve.

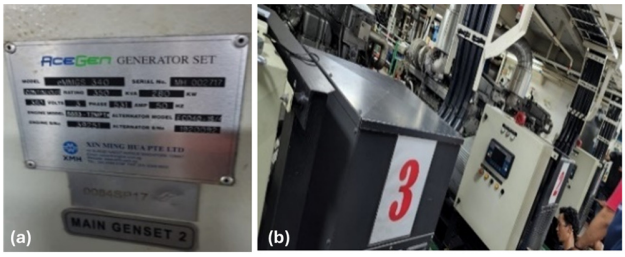

Fig. 7. Test generator: (a) generator nameplate and (b) generator installation in the ship's engine room.

The standard NSK 6318C3 generator bearing [40] was modified by applying a custom-fabricated porcelain insulation sleeve, approximately 2 mm thick (with specific thickness variations detailed in the experimental matrix), to the bearing's outer raceway (Figure 6(b)). The material was selected for its exceptional dielectric strength (withstanding up to 3000 V/mm) and high mechanical hardness. The installation required machining the bearing housing to accommodate the porcelain sleeve, as portrayed in Figure 8.

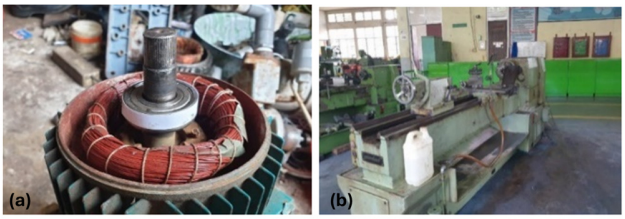

Fig. 8. Bearing modification process: (a) inserting the insulated bearing into the housing and (b) lathe used for precision machining of the bearing housing.

Data were collected on three key performance parameters: vibration, temperature, and electrical characteristics to holistically assess the impact of the insulation. Using ceramic insulation thicknesses varying from 2 mm to 3 mm, the aim was to determine the effect of thickness on vibration values and temperature changes. It should be noted that increased vibration indicates sparking in the bearing.

Vibration was measured using an oscilloscope at a single point on the Y-axis (vertical plane), as shown in Figure 9. This location was selected because the primary load from the rotating generator rotor is transmitted vertically through the bearing to the housing (Figure 8). Data were sampled every 2 s for two distinct scenarios: the baseline condition (non-insulated bearing) and the intervention condition (porcelain-insulated bearing).

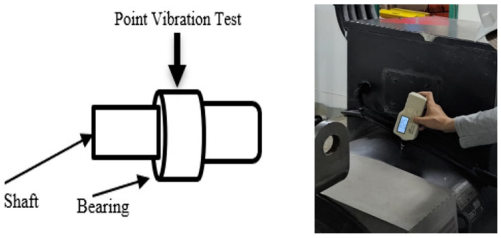

Fig. 9. Bearing vibration data collection point schematic.

The data collection techniques were:

- Operating Conditions: The generator was operated at its rated load of 22 kW. Vibration and amplitude data were recorded over a 1.8-s interval. The frequency range for amplitude measurement was set from 0 to 6000 Hz to capture relevant vibration signatures.
- Temperature Monitoring: The temperature of the bearing housing was monitored using a calibrated infrared thermometer. Readings were taken every 2 s, commencing 15 min after generator start-up to ensure thermal equilibrium and stable operating conditions.
- Electrical Parameters: Generator output voltage, current, and power were measured directly at the output terminals (Figures 10(a) and 10(b)) and verified against the control room monitor readings (Figure 10(c)) to ensure operational consistency.

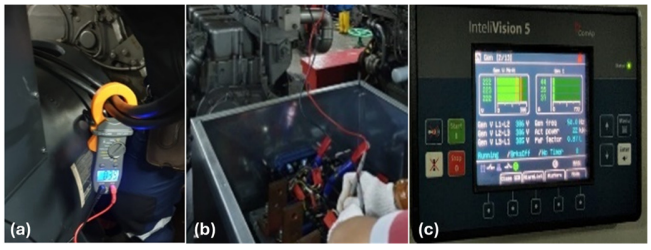

Fig. 10. Electrical data collection setup: (a) clamp meter placement for phase current measurement, (b) voltage measurement at the generator terminal block, and (c) electrical parameters displayed on the control monitor.

These concurrent measurements were critical for maintaining consistent operational benchmarks during data acquisition, thereby ensuring that any observed changes in vibration and temperature could be directly attributed to the bearing modification. The experimental procedure was systematically executed in three distinct phases. The Baseline Phase established a control dataset by operating the generator with a standard, non-insulated bearing at its rated load of 22 kW, 380 V, and 1500 rpm; vibration data were captured using a Fast Fourier Transform (FFT) analyzer, while bearing housing temperature and electrical current were recorded after a 15-min stabilization period. The Modification Phase involved halting the generator to replace the standard bearing with a modified unit equipped with a porcelain insulation sleeve, with thicknesses varied from 2 mm to 3 mm per experimental schedule. Finally, in the Intervention Phase, the generator was restarted under identical load and speed conditions, and the full suite of data parameters was collected again using the identical protocol and sampling intervals once the system had returned to a confirmed steady state.

The data were interrogated using multiple analytical techniques to comprehensively evaluate the intervention. Vibration analysis was conducted in both the time domain, observing amplitude fluctuations per (3) and (4), and the frequency domain using FFT to identify spectral changes between the baseline and intervention phases. Statistical analysis quantified the intervention's effectiveness through direct comparison and descriptive statistics, specifically tracking changes in the maximum, minimum, and mean values for vibration and temperature. Concurrently, thermal and electrical analysis involved comparing steady-state average temperature data and scrutinizing electrical parameters to confirm operational stability, thus verifying that the bearing insulation condition was the sole independent variable.

The success of the porcelain insulation was defined by three specific criteria. First, a significant reduction in vibration amplitude across both time and frequency domains was required, indicating the successful mitigation of EDM activity and its associated mechanical damage. Second, a marked decrease in the bearing's operating temperature was necessary to suggest reduced friction and lubricant degradation. Finally, the elimination of symptoms leading to premature failure, such as characteristic damage patterns in bearings or stator windings, served as the ultimate indicator of the solution's long-term efficacy and reliability.

III. RESULTS

This study demonstrates the efficacy of porcelain insulation in enhancing marine generator bearing performance, with significant improvements quantified across vibration, thermal, and electrical parameters.

1) Vibration Analysis

A comprehensive three-stage vibration analysis methodology was employed. First, overall vibration velocity (mm/s) and acceleration (mm/s²) were measured across the bearing assembly. Second, a detailed frequency spectrum analysis identified specific temporal (s) and characteristic frequency (Hz) shifts. Third, the statistical significance of these changes was confirmed. The collective results from these stages provide evidence of porcelain insulation's substantial impact on bearing dynamics.

The comparative vibration spectra, presented in Figures 11 and 12, along with corresponding data outlined in Tables I and II, visually and quantitatively illustrate a marked reduction in vibration time-domain fluctuations following insulation application. Furthermore, the amplitude spectra observed in Figures 13 and 14, with supporting data presented in Tables III and IV, reveal a pronounced attenuation of vibrational energy across the 1000 to 6000 Hz frequency range when the 2.00 mm porcelain insulation was installed.

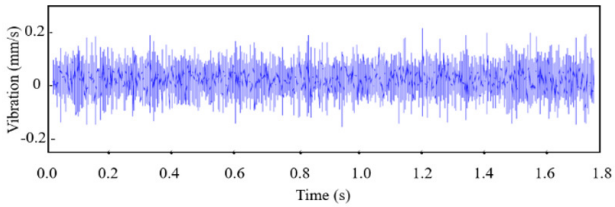

Fig. 11. Vibration spectrum of the baseline bearing without porcelain insulation.

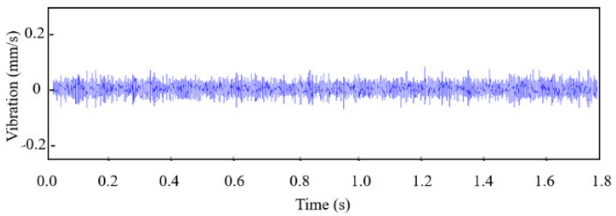

Fig. 12. Vibration spectrum of the bearing insulated with a 2.0 mm porcelain sleeve.

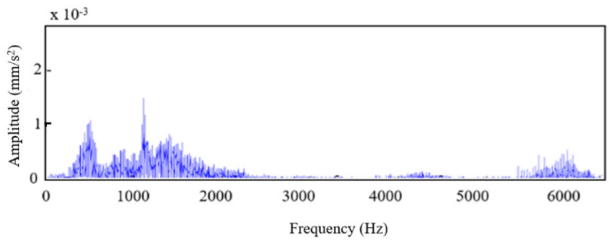

Fig. 13. Amplitude spectrum of the baseline bearing without porcelain insulation.

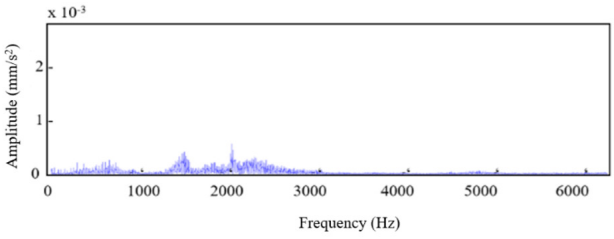

Fig. 14. Amplitude spectrum of the bearing insulated with a 2.0 mm porcelain sleeve.

TABLE I. TIME-DOMAIN VIBRATION FLUCTUATIONS OF THE NON-INSULATED BEARING AT 1500 rpm

Time (s)	Vibration (mm/s)
0.2	-0.1
0.4	0.1
0.6	-0.12
0.8	0.1
1.0	0.8
1.2	1.8
1.4	0.8
1.6	-0.6
1.8	1.6

TABLE II. TIME-DOMAIN VIBRATION FLUCTUATIONS OF THE PORCELAIN-INSULATED BEARING AT 1500 rpm

Time (s)	Vibration (mm/s)
0.2	-0.05
0.4	0.05
0.6	-0.04
0.8	0.03
1.0	0.05
1.2	0.03
1.4	0.05
1.6	-0.05
1.8	0.06

TABLE III. SPECTRAL AMPLITUDE VARIATIONS ACROSS 1000–6000 Hz FOR THE NON-INSULATED BEARING

Frequency (Hz)	Vibration $\times 10^{-3}$ (mm/s)
1000	0.5
2000	0.4
3000	0.2
4000	0.2
5000	0.1
6000	0.5

TABLE IV. SPECTRAL AMPLITUDE VARIATIONS ACROSS 1000–6000 Hz FOR THE BEARING WITH 2.0 mm PORCELAIN INSULATION

Frequency (Hz)	Vibration $\times 10^{-3}$ (mm/s)
1000	0.01
2000	0.3
3000	0.01
4000	0.01
5000	0.01
6000	0.01

2) Changes in Temperature

The generator bearing temperature profile was carefully monitored under operational conditions. Before insulation, the bearing exhibited a higher and less stable thermal profile, with temperatures reaching 43.3 °C. After the application of porcelain insulation, a much more stable and lower temperature behavior was recorded, with a stable operational temperature of 39.6 °C. This represents a significant temperature reduction of 3.7 °C.

This reduction stems from the effective mitigation of arc currents. Previously, these currents generated excessive heat through localized discharges and Joule heating within the bearing assembly. By acting as a very high-resistance barrier (measured at 1000 GΩ), the porcelain insulation interrupts the flow of these parasitic currents, eliminating the primary heat source and improving the system's thermal stability. This correlation confirms that the temperature reduction is not coincidental, but rather a direct consequence of suppressing electrical energy dissipation within the bearing, ultimately improving lubrication integrity and reducing mechanical wear.

3) Electrical Parameters

The implementation of porcelain insulation fundamentally altered the generator's electrical characteristics by establishing high-resistance isolation between the rotor shaft and generator frame. This critical modification disrupted the circulation path for parasitic bearing currents, as quantitatively demonstrated by an insulation resistance measurement of 1000 GΩ. This effectively created an open circuit for damaging currents, preventing shaft voltage potential from discharging through the bearings, and thereby eliminating the fundamental mechanism responsible for electrical arcing and associated damage.

These electrical improvements yielded significant enhancements in overall generator performance and efficiency. The elimination of energy dissipation from Joule heating and electrical arcing resulted in more stable output voltage characteristics with reduced harmonic distortion. This electrical stability is further reinforced by diminished non-linear loading effects. The previously documented reductions in mechanical vibration and operating temperature provide additional evidence of suppressed parasitic energy losses, indicating measurable improvements in operational efficiency

Consequently, the generator maintains rated power output with greater stability, substantially enhancing its reliability for supporting critical marine electrical systems.

4) Anomalies and Unexpected Results

The implementation of porcelain insulation introduced no critical anomalies or adverse operational effects. The insulation system did not generate significant capacitive coupling issues or compromise rotor dynamic balance. The sole mechanical requirement precision machining of the bearing housing to accommodate the porcelain layer was anticipated during the design phase. Electrically, the system performed within expected parameters without voltage spikes or instability throughout testing. The solution, therefore, demonstrated robust performance in eliminating bearing arcing while introducing no new failure modes or operational deficiencies

IV. DISCUSSION

The experimental results demonstrate porcelain ceramic insulation's efficacy as a superior mitigation strategy against bearing currents and fluting damage in marine generators. The 93.75% vibration reduction and 3.7 °C temperature decrease represent quantitative evidence of successful parasitic current path interruption, not merely statistical improvements.

TABLE V. VIBRATION DAMPING EFFECTIVENESS BASED ON CERAMIC INSULATION THICKNESS VARIATION (ON NSK 6318C3 BEARING, OPERATING CONDITION 1500 rpm, 22 kW)

Data	Ceramic isolation thickness (mm)	Vibration velocity - RMS (mm/s)	Vibration amplitude – peak (mm/s^2)	Vibration damping (%)	Amplitude damping (%)	Information
1	0.00	0.80	0.012	Baseline	Baseline	Condition without isolation (baseline). High vibration due to electric arcing.
2	2.00	0.05	0.0007	93.75	94.17	Optimal thickness from research. Very effective damping and perfect isolation electricity.
3	2.05	0.049	0.00068	93.88	94.33	Very similar performance with 2.00 mm. Variation in manufacturing tolerance.
4	2.15	0.048	0.00066	94.00	94.50	Damping was slightly better. Thickness addition increased stiffness and mass damping.
5	2.20	0.047	0.00065	94.13	94.58	Damping shows an increasing trend. The ideal point before excessive mass addition.
6	2.75	0.055	0.0008	93.13	93.33	Damping decreased. Excessive thickness caused too much mass, potentially changing the dynamic system's characteristics and lowering its effectiveness .

These findings corroborate and extend previous research in [23, 41], regarding CMV and capacitive coupling origins of bearing currents. However, conventional solutions, like shaft grounding [33] or insulated bearings [34], prove inadequate in marine environments characterized by salt contamination, high humidity, and mechanical stress. The external porcelain insulation solution developed in this study addresses these limitations through a permanent, maintenance-free dielectric barrier essential for maritime reliability.

The temperature reduction mechanism operates through two primary pathways: elimination of discharge-induced thermal erosion, as identified in [10], and restoration of lubricant integrity through reduced electro-thermal degradation, as observed in [42]. This dual mechanism reduces mechanical friction while enhancing heat dissipation efficiency.

Vibration spectrum analysis provided further validation, showing the disappearance of high-frequency components and amplitude stabilization, indicating suppression of electrical enables extended generator service life, reduced operational downtime, and enhanced vessel safety, establishing a new performance paradigm that surpasses conventional mitigation methods.

The current research delivers both technical validation of ceramic-based mitigation and substantial practical advancement for maritime engineering. Porcelain insulation implementation EDM impulses and micro-pitting. This confirms the insulation's effectiveness in preventing fluting and frosting damage [7, 30].

Critical to implementation is thickness optimization. The data presented in Tables V and VI indicate optimal performance at approximately 2.20 mm, beyond which effectiveness declines due to rotodynamic considerations. Excessive mass addition alters natural frequency characteristics, potentially introducing imbalance, establishing insulator thickness as both an electrical and dynamic design parameter. Practically, this solution offers non-intrusive retrofitting capability. Unlike fundamental redesign approaches [25], bearing housing insulation enables implementation on existing generators without core modifications, presenting an economically viable solution for fleet-wide application.

While promising, this study's scope is limited to a single generator type under specific load conditions. Future research should investigate long-term endurance under varied operational profiles, including transient and overload conditions. The exploration of alternative composite materials offering comparable dielectric strength with reduced mass presents another valuable research direction.

TABLE VI. INFLUENCE THICKNESS ISOLATION CERAMICS TO CHANGE TEMPERATURE BEARINGS (ON NSK 6318C3 BEARING , OPERATING CONDITION 1500 rpm, 22 kW)

Data	Ceramic isolation thickness (mm)	Operating temperature (°C)	Temperature decline (°C)	Temperature decline (%)	Information
1	0.00	43.3	0.0	0.0	Baseline condition without insulation. High temperature resulting from warmup due to electric arcing and mechanical friction.
2	2.00	39.7	3.6	8.3	Optimal thickness from research. Significant temperature decline due to elimination of heat source from electric arcing.
3	2.05	39.6	3.7	8.5	Similar performance decline to 2.00 mm. Electrical isolation effect remains dominant.
4	2.15	39.5	3.8	8.8	Optimal temperature reduction. The ideal combination of electrical isolation and thermal insulation.
5	2.20	39.6	3.7	8.5	Decline starts stable. Additional thickness provides a minimal thermal insulation effect.
6	2.75	40.2	3.1	7.2	Effectiveness decline. Excessive thickness withhold heat inside the bearing assembly, reducing heat dissipation to the environment.

TABLE VII. COMPARISON OF 10 STUDIES RELATED TO BEARINGS AND ELECTRIC CURRENT MITIGATION

Researcher (Year)		**Title / Focus**	**Methodology**	**Types of solutions studied**	**Excess**	**Disadvantages / Limitations**	**Difference with our research**
1	[41]	Bearing currents and their relationship to PWM drives.	Theoretical & experimental analysis.	Understanding base mechanism bearing current on PWM motor.	Foundational research that forms a key reference.	Not offering practical solution in a specific way.	We focus on marine generators (not PWM motors) and offer practical solution (isolation ceramics), not just problem analysis.
2	[43]	Influence of motor operating parameters on discharge bearing current activity.	Controlled laboratory experiment.	Analysis of operating parameters (speed , voltage).	Detailed quantification of operational parameter influence.	Laboratory-scale only. No system-level integration issues.	We implement solutions in the real-world environment (training ship) and measure its overall impact on system reliability.
3	[10]	Damages on lubricated surfaces in bearings under weak electrical currents.	Material experiments and SEM analysis.	Understanding the impact of weak microscopic currents on the surface.	Analysis of deep material degradation.	The analysis is highly material-specific and does not discuss macro-scale engineering solutions.	Our research is in applied engineering, directly implementing a solution to prevent damage analyzed.
4	[8]	Analytical determination of the winding-to-rotor capacitance.	Analytical and numerical modeling.	Mathematical model for predicting shaft tension.	An elegant approach for early prediction.	The model can become complex and requires specific machine parameters.	We avoid modeling complexity with a direct solution and an easy physical implemented (ceramic insulator).
5	[44]	On the Application of Extended Grounded Slot Electrodes	simulation and validation experiment	Grounded Slot Electrodes (Active solution / motor modification)	Effective solutions at the motorcycle design level	Need modification expensive and unsuitable stator design practical for motorbikes that have installed	outer isolator is non- intrusive and retrofittable, can applied to generators that have been operate without modification big
6	[16]	Experimental ball bearing impedance analysis.	Bearing impedance experiment.	Understanding the electrical characteristics of bearings.	Impedance data is essential for accurate modeling.	Contribution focuses more on fundamental understanding base than on solution practical.	We use this fundamental understanding to develop direct, practical solutions that overcome empedance-related problems.
7	[23]	A review of modeling and mitigation techniques.	Paper review	Conduct a comprehensive review of various techniques.	Very extensive and informative coverage.	As a review paper, does not present original experimental contributions or novel solutions.	Our research consists of empirical implementation and validation of a mitigation strategy identified in a prior review paper.
8	[45]	Novel technique of vibration minimization.	Experiments on machining systems.	General techniques for minimizing vibration.	Applications in different fields (machining) demonstrate the universalityof vibration-related problems.	Their solution is specific to machining systems and is not designed for electrical bearing currents in generators.	We specifically target a unique vibration source, namely electrical current, as opposed to general mechanical vibration.
9	[46]	Measurement of direct current voltage causing electrical pitting	Laboratory experiment to determine the threshold voltage.	Setting the critical voltage limit that causes damage.	The threshold dara is critical for system design.	Focus on the cause, not on the cure or prevention.	Our research addresses problems after they occur (or proactively to prevent them) by providing solutions, not just by defining the issues.
10	[42]	Influence of electric discharge activity on bearing grease.	Analysis chemistry and properties of grease.	Impact release load on grease degradation.	Impact with no direct current, frequent electricity ignored..	Just analyzing grease degradation, not solution systemic.	We prevent grease degradation by eliminating the primary source (arcing), thereby protecting all over system bearings.

V. CONCLUSIONS

This study demonstrates that applying porcelain ceramic insulation to marine generator bearing housings provides an effective solution for mitigating bearing currents and preventing fluting damage. The experimental results address the three primary research objectives: First, insulator thickness significantly influences system performance, with an optimal 2.20 mm configuration achieving 94.13% vibration damping and a 3.7 °C temperature reduction, while excessive thickness adversely affects rotodynamic stability. Second, the porcelain's ultra-high resistivity (1,000 GΩ) completely disrupts parasitic current paths, eliminating Electrical Discharge Machining (EDM) that causes surface erosion, micro-pitting, and fluting damage, as confirmed by vanished high-frequency components in vibration spectra. Third, the solution demonstrates practical feasibility through its robust, non-intrusive design that withstands harsh maritime conditions without maintenance, requiring only straightforward bearing housing modifications for cost-effective fleet retrofitting.

ACKNOWLEDGMENT

The Authors acknowledge the support of Merchant Marine Polytechnic of Makassar, by the training ship KL. Sultan Hasanuddin which provided data from the survey, observation and interview the crews.

REFERENCES

[1] S. S. H. Bukhari, G. J. Sirewal, F. A. Chachar, and J.-S. Ro, "Dual-Inverter-Controlled Brushless Operation of Wound Rotor Synchronous Machines Based on an Open-Winding Pattern," *Energies*, vol. 13, no. 9, 2020, Art. no. 2205, https://doi.org/10.3390/en13092205.

[2] A. Duda and P. Drozdowski, "Induction Motor Fault Diagnosis Based on Zero-Sequence Current Analysis," *Energies*, vol. 13, no. 24, Dec. 2020, Art. no. 6528, https://doi.org/10.3390/en13246528.

[3] A. Zorig, S. Hedayati Kia, A. Chouder, and A. Rabhi, "A comparative study for stator winding inter-turn short-circuit fault detection based on harmonic analysis of induction machine signatures," *Mathematics and Computers in Simulation*, vol. 196, pp. 273–288, 2022, https://doi.org/10.1016/j.matcom.2022.01.019.

[4] I. Issaadi, K. E. Hemsas, and A. Soualhi, "Wind turbine gearbox diagnosis based on stator current," *Energies*, vol. 16, no. 14, 2023, Art. no. 5286, https://doi.org/10.3390/en16145286.

[5] M. L. Swarupa, K. Rayudu, C. S. Kumar, S. L. Gundebommu, and P. Kamalakar, "Machine Learning Techniques for Power Quality Enhancement of Power Distribution Systems with FACTS Devices," *Engineering, Technology & Applied Science Research*, vol. 14, no. 4, pp. 14939–14944, Aug. 2024, https://doi.org/10.48084/etasr.7233.

[6] R. N. Toma, A. E. Prosvirin, and J.-M. Kim, "Bearing Fault Diagnosis of Induction Motors Using a Genetic Algorithm and Machine Learning Classifiers," *Sensors*, vol. 20, no. 7, 2020, Art. no. 1884, https://doi.org/10.3390/s20071884.

[7] K. Esmaeili, L. Wang, T. J. Harvey, N. M. White, and W. Holweger, "Electrical Discharges in Oil-Lubricated Rolling Contacts and Their Detection Using Electrostatic Sensing Technique," *Sensors*, vol. 22, no. 1, 2022, Art. no. 392, https://doi.org/10.3390/s22010392.

[8] J. O. Stockbrügger and B. Ponick, "Analytical Determination of the Slot and the End-Winding Portion of the Winding-to-Rotor Capacitance for the Prediction of Shaft Voltage in Electrical Machines," *Energies*, vol. 14, no. 1, 2021, Art. no. 174, https://doi.org/10.3390/en14010174.

[9] Y.-C. Chiou, R.-T. Lee, and S.-M. Lin, "Formation mechanism of electrical damage on sliding lubricated contacts for steel pair under DC electric field," *Wear*, vol. 266, no. 1-2, pp. 110–118, Jan. 2009, https://doi.org/10.1016/j.wear.2008.06.001.

[10] G. Xie, J. Luo, D. Guo, S. Liu, and G. Li, "Damages on the lubricated surfaces in bearings under the influence of weak electrical currents," *Science China Technological Sciences*, vol. 56, no. 12, pp. 2979–2987, Dec. 2013, https://doi.org/10.1007/s11431-013-5399-7.

[11] A. R. S. Queiroz, E. C. Senger, L. C. L. Queiroz, E. Rangel, and V. S. de Paula, "Maintenance Strategy for Electrical Equipment Based on Integrated Operations," *IEEE Transactions on Industry Applications*, vol. 53, no. 3, pp. 3189–3197, 2017, https://doi.org/10.1109/TIA.2016.2645689.

[12] G. Barone, A. Buonomano, G. Del Papa, R. Maka, and A. Palombo, "How to achieve energy efficiency and sustainability of large ships: a new tool to optimize the operation of on-board diesel generators," *Energy*, vol. 282, Nov. 2023, Art. no. 128288, https://doi.org/10.1016/j.energy.2023.128288.

[13] V. J. Jimenez, H. Kim, and Z. H. Munim, "A review of ship energy efficiency research and directions towards emission reduction in the maritime industry," *Journal of Cleaner Production*, vol. 366, Sept. 2022, Art. no. 132888, https://doi.org/10.1016/j.jclepro.2022.132888.

[14] K. Alewine and W. Chen, "A review of electrical winding failures in wind turbine generators," *IEEE Electrical Insulation Magazine*, vol. 28, no. 4, pp. 8–13, July 2012, https://doi.org/10.1109/MEI.2012.6232004.

[15] J. Kluss, M. R. Chalaki, W. Whittington, H. Rhee, S. Whittington, and A. Yadollahi, "Porcelain insulation – defining the underlying mechanism of failure," *High Voltage*, vol. 4, no. 2, pp. 81–88, 2019, https://doi.org/10.1049/hve.2019.0004.

[16] D. De Gaetano, W. Zhu, X. Sun, X. Chen, A. Griffo, and G. W. Jewell, "Experimental Ball Bearing Impedance Analysis Under Different Speed and Electrical Conditions," *IEEE Transactions on Dielectrics and Electrical Insulation*, vol. 30, no. 3, pp. 1312–1321, June 2023, https://doi.org/10.1109/TDEI.2023.3271958.

[17] G. Dilev, B. Ose-Zala, and E. Jakobson, "Self-Excitation of Low-Speed Inductor Generator," *Latvian Journal of Physics and Technical Sciences*, vol. 49, no. 4, 2012, Art. no. 21, https://doi.org/10.2478/v10047-012-0020-6.

[18] A. Trentin *et al*., "Research and Realization of High-Power Medium-Voltage Active Rectifier Concepts for Future Hybrid-Electric Aircraft Generation," *IEEE Transactions on Industrial Electronics*, vol. 68, no. 12, pp. 11684–11695, Dec. 2021, https://doi.org/10.1109/TIE.2020.3040692.

[19] S.-T. Wu and C.-H. Han, "Design and Implementation of a Full-Bridge LLC Converter With Wireless Power Transfer for Dual Mode Output Load," *IEEE Access*, vol. 9, pp. 120392–120406, 2021, https://doi.org/10.1109/ACCESS.2021.3107868.

[20] L. Pirashanthiyah, H. N. Edirisinghe, W. M. P. De Silva, S. R. A. Bolonne, V. Logeeshan, and C. Wanigasekara, "Design and Analysis of a Three-Phase Interleaved DC-DC Boost Converter with an Energy Storage System for a PV System," *Energies*, vol. 17, no. 1, 2024, Art. no. 250, https://doi.org/10.3390/en17010250.

[21] I. Kerszenbaum, "Shaft currents in electric machines fed by solid-state drives," *in 1992 IEEE Conference Record of the Industrial and Commercial Power Systems Technical Conference*, Pittsburgh, Pennsylvania, May 1992, pp. 71–79, https://doi.org/10.1109/ICPS.1992.163388.

[22] G. Zaleskis and I. Rankis, "Capacitor activated self-excitation system of synchronous generator," Electronics and Electrical Engineering, vol. 123, no. 7, pp. 53–57, July 2012, https://doi.org/10.5755/j01.eee.123.7.2373.

[23] W. Zhu, D. De Gaetano, X. Chen, G. W. Jewell, and Y. Hu, "A Review of Modeling and Mitigation Techniques for Bearing Currents in Electrical Machines With Variable-Frequency Drives," *IEEE Access*, vol. 10, pp. 125279–125297, 2022, https://doi.org/10.1109/ACCESS.2022.3225119.

[24] A. Loulijat *et al*., "Application and Comparison of a Modified Protection Scheme Utilizing a Proportional–Integral Controller with a Conventional Design to Enhance Doubly Fed Induction Generator Wind Farm Operations during a Balanced Voltage Dip," *Processes*, vol. 11, no. 10, 2023, Art. no. 2834, https://doi.org/10.3390/pr11102834.

[25] A. U. Rehman *et al*., "Efficient Fault Detection of Rotor Minor Inter-Turn Short Circuit in Induction Machines Using Wavelet Transform and

Empirical Mode Decomposition," *Sensors*, vol. 23, no. 16, 2023, Art. no. 7109, https://doi.org/10.3390/s23167109.

[26] K. S. Chatra, J. A. Osara, and P. M. Lugt, "Impact of grease churning on grease leakage, oil bleeding and grease rheology," *Tribology International*, vol. 176, Dec. 2022, Art. no. 107926, https://doi.org/10.1016/j.triboint.2022.107926.

[27] J. Drabik, R. Kozdrach, and M. Szczerek, "Characterization of nano-silica vegetable grease with diffusing wave spectroscopy DWS and Raman spectroscopy," *Scientific Reports*, vol. 13, no. 1, Nov. 2023, Art. no. 18989, https://doi.org/10.1038/s41598-023-45669-0.

[28] F. Schwack, N. Bader, J. Leckner, C. Demaille, and G. Poll, "A study of grease lubricants under wind turbine pitch bearing conditions," *Wear*, vol. 454–455, Aug. 2020, Art. no. 203335, https://doi.org/10.1016/j.wear.2020.203335.

[29] N. Khan *et al.*, "A time fractional model of a Maxwell nanofluid through a channel flow with applications in grease," *Scientific Reports*, vol. 13, no. 1, 2023, Art. no. 4428, https://doi.org/10.1038/s41598-023-31567-y.

[30] V. V. Bryukhovetsky *et al.*, "Formation mechanism of craters on the surface of AA6111 aluminum alloy irradiated by quasi-relativistic high-current electron beam," *Vacuum*, vol. 215, Sept. 2023, Art. no. 112263, https://doi.org/10.1016/j.vacuum.2023.112263.

[31] H. N. Kaufman and J. Boyd, "The Conduction of Current in Bearings," A S L E Transactions, vol. 2, no. 1, pp. 67–77, 1959, https://doi.org/10.1080/05698195908972359.

[32] V. B. M. Krishna and V. Sandeep, "Experimental Investigations on Loading Capacity and Reactive Power Compensation of Star Configured Three Phase Self Excited Induction Generator for Distribution Power Generation," *Distributed Generation & Alternative Energy Journal*, vol. 37, no. 3, pp. 725–748, Feb. 2022, https://doi.org/10.13052/dgaej2156-3306.37316.

[33] J. A. Davidson and A. K. Mishra, "Surface Modification Issues for Orthopaedic Implant Bearing Surfaces," *Materials and Manufacturing Processes*, vol. 7, no. 3, pp. 405–421, 1992, https://doi.org/10.1080/10426919208947429.

[34] B. S. Bal, J. Garino, M. Ries, and M. N. Rahaman, "A Review of Ceramic Bearing Materials in Total Joint Arthroplasty," *HIP International*, vol. 17, no. 1, pp. 21–30, 2007, https://doi.org/10.1177/112070000701700105.

[35] Z. Li, K. Yang, J. Chen, and S. Duan, "A Novel Fault Identification Method Using Modified Morphological Denoising via Structuring Element Optimization for Transmission Systems of Shipborne Antennas," *Journal of Marine Science and Engineering*, vol. 10, no. 2, Art. no. 190, 2022, https://doi.org/10.3390/jmse10020190.

[36] R. W. Rice, C. Cm. Wu, and F. Boichelt, "Hardness‐Grain‐Size Relations in Ceramics," *Journal of the American Ceramic Society*, vol. 77, no. 10, pp. 2539‐2553, 1994, https://doi.org/10.1111/j.1151-2916.1994.tb04641.x.

[37] M. Touzin, D. Goeuriot, C. Guerret-Piécourt, D. Juvé, and H.-J. Fitting, "Alumina based ceramics for high-voltage insulation," *Journal of the European Ceramic Society*, vol. 30, no. 4, pp. 805–817, Mar. 2010, https://doi.org/10.1016/j.jeurceramsoc.2009.09.025.

[38] G. V. Sarrigani and I. S. Amiri, "Introduction to Glass and Glass-Ceramic Background," *in Willemite-Based Glass Ceramic Doped by Different Percentage of Erbium Oxide and Sintered in Temperature of 500-1100C: Physical and Optical Properties*, G. V. Sarrigani and I. S. Amiri, Eds. Cham: Springer International Publishing, 2019, ch. 1, pp. 1–11.

[39] D. E. Quesada, L. P. Villarejo, and P. S. Soto, "Introductory Chapter: Ceramic Materials - Synthesis, Characterization, Applications and Recycling," *in Ceramic Materials: Synthesis, Characterization, Applications and Recycling,* D. E. Quesada, L. P. Villarejo, and P. S. Soto, Eds., London, United Kingdom: IntechOpen, 2019, ch. 1, pp. 1–4.

[40] SKF Australia, "SKF Bearings," *SKF*, Gothenburg, pp. 1–3, https://www.skf.com/au/products/rolling-bearings/ball-bearings/deep-groove-ball-bearings/productid-6218-2Z%2FC3.

[41] D. Busse, J. Erdman, R. J. Kerkman, D. Schlegel, and G. Skibinski, "Bearing currents and their relationship to PWM drives," *IEEE Transactions on Power Electronics*, vol. 12, no. 2, pp. 243–252, 1997, https://doi.org/10.1109/63.558735.

[42] A. Romanenko, J. Ahola, and A. Muetze, "Influence of electric discharge activity on bearing lubricating grease degradation," *in 2015 IEEE Energy Conversion Congress and Exposition (ECCE)*, Montreal, Canada, Sept. 2015, pp. 4851–4852, https://doi.org/10.1109/ECCE.2015.7310344.

[43] A. Muetze, J. Tamminen, and J. Ahola, "Influence of Motor Operating Parameters on Discharge Bearing Current Activity," *IEEE Transactions on Industry Applications*, vol. 47, no. 4, pp. 1767–1777, July 2011, https://doi.org/10.1109/TIA.2011.2154353.

[44] K. Vostrov, J. Pyrhönen, M. Niemelä, P. Lindh, and J. Ahola, "On the Application of Extended Grounded Slot Electrodes to Reduce Noncirculating Bearing Currents," *IEEE Transactions on Industrial Electronics*, vol. 70, no. 3, pp. 2286–2295, Mar. 2023, https://doi.org/10.1109/TIE.2022.3172748.

[45] A. D. Apte *et al.*, "Novel technique of vibration minimization during hard machining," *Engineering Reports*, vol. 6, no. 8, 2024, Art. no. e12811, https://doi.org/10.1002/eng2.12811.

[46] S. Noguchi, S.-N. Kakinuma, and T. Kanada, "Measurement of direct current voltage causing electrical pitting," *Journal of Advanced Mechanical Design, Systems, and Manufacturing*, vol. 4, no. 6, pp. 1084–1094, 2010, https://doi.org/10.1299/jamdsm.4.1084.